HHS Public Access

Author manuscript

Nucl Med Biol. Author manuscript; available in PMC 2016 April 01.

Published in final edited form as:

Nucl Med Biol. 2015 April ; 42(4): 375–380. doi:10.1016/j.nucmedbio.2014.12.012.

Radiolabeled Antibodies in Prostate Cancer: A Case Study Showing the Effect of Host Immunity on Antibody Bio-distribution

Oskar Vilhelmsson-Timmermand[1], **Elmer Santos**[2], **Daniel LJ Thorek**[3], **Susan Evans-Axelsson**[4], **Anders Bjartell**[4], **Hans Lilja**[5,6,7,8], **Steven M Larson**[2], **Sven-Erik Strand**[1], **Thuy A. Tran**[1,9], and **David Ulmert**[5,10]

[1]Department of Medical Radiation Physics, Lund University, Lund, Sweden

[2]Department of Radiology (Nuclear Medicine Service), Memorial Sloan-Kettering Cancer Center, New York, NY, USA

[3]Department of Radiology and Radiological Sciences, Division of Nuclear Medicine, The Johns Hopkins University School of Medicine, Baltimore, MD, USA

[4]Department of Clinical Sciences, Division of Urological Cancers, Lund University, Malmö, Sweden

[5]Department of Surgery (Urology), Memorial Sloan-Kettering Cancer Center, New York, NY, USA

[6]Departments of Laboratory Medicine and Medicine (GU Oncology), Memorial Sloan-Kettering Cancer Center, New York, NY, USA

[7]Nuffield Department of Surgical Sciences, University of Oxford, Oxford, United Kingdom

[8]Department of Laboratory Medicine, Lund University, Malmö, Sweden

[9]Lund University Bioimaging Center, Lund University, Lund, Sweden

[10]Department of Clinical Sciences, Division of Urological Research, Lund University, Malmö, Sweden

Abstract

Objectives—Human tumors xenografted in immunodeficient mice are crucial models in nuclear medicine to evaluate the effectiveness of candidate diagnostic and therapeutic compounds. However, little attention has been focused on the biological profile of the host model and its potential effects on the bio-distribution and tumor targeting of the tracer compound under study. We specifically investigated the dissimilarity in bio-distribution of ^{111}In-DTPA-5A10, which targets free Prostate Specific Antigen (fPSA), in two animal models.

Methods—*In vivo* bio-distribution studies of ^{111}In-DTPA-5A10 were performed in immunodeficient BALB/c-nu or NMRI-nu mice with subcutaneous (s.c.) LNCaP tumors. Targeting-specificity of the tracer was assessed by quantifying the uptake in (a) mice with s.c. xenografts of PSA-negative DU145 cells as well as (b) BALB/c-nu or NMRI-nu mice co-injected with an excess of non-labeled 5A10. Finally, the effect of neonatal Fc-receptor (FcRn) inhibition on the bio-distribution of the conjugate was studied by saturating FcRn-binding capacity with nonspecific IgG1.

Results—The inherent biological attributes of the mouse model substantially influenced the bio-distribution and pharmacokinetics of ^{111}In-DTPA-5A10. With LNCaP xenografts in BALB/c-nu mice (with intact B and NK cells but with deficient T cells) versus NMRI-nu mice (with intact B cells, increased NK cells and absent T cells), we observed a significantly higher hepatic accumulation (26±3.9 versus 3.5±0.4 %IA/g respectively), and concomitantly lower tumor uptake (25±11 versus 52±10 %IA/g respectively) in BALB/c-nu mice. Inhibiting FcRn by administration of nonspecific IgG1 just prior to ^{111}In-DTPA-5A10 did not change tumor accumulation significantly.

Conclusions—We demonstrated that the choice of immunodeficient mouse model importantly influence the bio-distribution of ^{111}In-DTPA-5A10. This study further highlighted important considerations in the evaluation of preclinical tracers, with respect to gaining information on their performance in the translational setting. Investigators utilizing xenograft models need to assess not only radiolabeling strategies, but also the host immunological status.

1. Introduction

There is an urgent need for molecular imaging methods to sensitively and accurately detect and monitor aggressive forms of prostate cancer. Initially proposed over half a century ago, radiolabeled antibodies successfully target tumor-specific molecules and provide an attractive platform for non-invasive *in vivo* imaging in nuclear medicine. Radiolabeled antibodies, with high affinity for antigens that are either disease-specific or overexpressed in disease states, accumulate at disease sites. This activity can be measured by planar or tomographic imaging [1]. Continual refinements in instrumentation, antibody production and radiochemistry over the intervening decades have made antibody imaging one of the most promising tools for staging and monitoring disseminated prostate cancer (PCa).

While many novel radiotracers have been developed for the screening and diagnosis of prostate cancer, translation into clinical practice has proven challenging. Candidate molecules often accrue through the *in vitro* screening of species-specific proteins that are up-regulated in human cancer cell lines. Subsequently, tumor-specific accumulation of a tracer in subcutaneous and homogeneous antigen-positive xenografts in immune deficient mice is regarded as preclinical evidence of success. The definition of tumor-specific uptake is often based on criteria which focus on the significantly lower uptake in tumors deprived of the targeted protein, or tumors in which the radiolabeled tracer has been successfully blocked by an excess of unlabeled compound.

Studies of antibody elimination in rodents have shown that clearance is depending on immunodeficiency profile and endogenous levels of antibodies [2,3]. Surprisingly little

attention has been paid to the potential impact of the immunological profile of the host model on tumor uptake of the tracer, and the possible effects this may have on the critical outcomes of bio-distribution and tumor targeting.

Recently, members of our research group reported on the development of a Zirconium-89 labeled PET tracer, ^{89}Zr-DFO-5A10, which specifically targets a unique epitope only available on free (uncomplexed) forms of Prostate Specific Antigen, fPSA [4]. PSA is an androgen-regulated kallikrein-related serine protease that is exclusively expressed in human prostatic epithelial tissue, including malignantly deranged forms [5]. PSA is best known for its use as a blood biomarker for prostate cancer [6] in humans and naturally deficient in mice [7]. Approximately, only one millionth of the PSA present in prostate epithelium is normally released into the blood [8,9]. Upon reaching the perivascular space, a predominant proportion of PSA is covalently and irreversibly bound to abundant extracellular proteinase inhibitors and converted to a non-catalytic complexed form (complexed PSA, cPSA) [10]. By employing a probe that specifically recognizes a unique epitope overlapping the catalytic cleft of PSA that is not available on complexed PSA [11,12]. Thus, the complexed forms of PSA in blood are excluded from being targeted.

Here, we utilized an ^{111}In-labeled 5A10 mouse antibody to investigate the potential influence of mouse models on the kinetics and bio-distribution of tracers. Human prostate cancer cell lines (LNCaP, DU145) were subcutaneously inoculated into two commonly-employed immunodeficient mouse strains: (a) NMRI-nu mice, characterized as athymic with a very low T cell population that respond poorly to T cell-dependent antigen presentation; (b) BALB/c-nu mice, also regarded as athymic but with no T cell population. Both strains have intact B cells with antibody response confined to IgM class. Both strains have natural killer (NK) cells intact. However, the level of NK cells in NMRI-nu mice is particularly increased in comparison to normal NMRI mice.

Our results highlight the importance of mouse models, in particular the immunological competence (or lack thereof), in the interpretation of pre-clinical targeted imaging experiments in general.

2. MATERIALS AND METHODS

All reagents were purchased from Thermo Scientific, unless otherwise stated.

2.1. Conjugation and radiolabeling

5A10, the murine IgG1, (provided by the University of Turku, Finland)was conjugated with the chelator CHX-A”-DTPA (Macrocyclics Inc.) as follows: A solution of 5A10 in PBS was adjusted to pH 9.2 using 0.07 M sodium borate buffer (Sigma Aldrich), and thereafter concentrated on an Amicon Ultra-2 centrifugal filter (2 mL, 100 K; Millipore). The chelator compound CHX-A”-DTPA was then added to the protein solution in a molar ratio of 3:1 (chelator to antibody), and incubated with gentle shaking at 40 °C. The reaction was terminated after 4 h. The next step was separating CHX-A”-DTPA-5A10, hereafter referred to as DTPA-5A10, from the free chelator by size-exclusion chromatography on a NAP-5 column (GE Healthcare) equilibrated with 20 mL 0.2 M ammonium acetate buffer, pH 5.5.

Finally, conjugated 5A10 was eluted with 1 mL ammonium acetate buffer and aliquot samples were stored at -20 °C.

For radiolabeling, typically 300 μg DTPA-5A10 (1 μg/μL in 0.2 M ammonium acetate buffer, pH 5.5) was mixed with a predetermined amount (~ 15 MBq) of $^{111}InCl_3$ (Mallinkrodt Medical). After incubating the mixture at room temperature for 1.5–2 h, the labeling was terminated and the radiotracer purified on a NAP-5 column, equilibrated with PBS. Labeling efficiency and kinetics were monitored with instant thin layer chromatography (Biodex), eluted with 0.2 M citric acid (Sigma Aldrich). In this system, the radiolabeled conjugate remains at the origin line, while free ^{111}In migrates with the front of the solvent. The radioactive distribution was determined with a Cyclone Storage Phosphor System using the Optiquant quantification software (both from Perkin Elmer).

2.2. In vitro stability studies

To assess the stability of the radio-immunoconjugate ^{111}In-DTPA-5A10, the compound was incubated in triplicate at 37°C in murine serum from NMRI-nu (Taconic) and BALB/c-nu mice (Charles River), respectively. 10 μL of DTPA-5A10 was mixed with 100 μL of each strain's mouse serum. Approximately 20 μL of each sample was collected from the two DTPA-5A10 mixtures at 2, 3 and 9 days of incubation and analyzed by SDS-PAGE on NuPAGE 4–12% Bis-Tris gel (Invitrogen) in MES buffer (200 V constant, ~ 50 min). ^{111}In-DTPA and free ^{111}In diluted in PBS were run in parallel with the incubated sample as controls. The distribution of the samples along the gel was evaluated using Cyclone Storage Phosphor System (Perkin Elmer).

2.3. Cell lines

PSA-expressing LNCaP and control DU145 (PSA-negative) cell lines were purchased from the American Type Culture Collection. Cells were cultured in RPMI 1640 medium enriched with 10% fetal bovine serum, to which penicillin 100 IU/mL and 100 μg/mL streptomycin were added. The cells were maintained at 37°C in a humidified incubator at 5% CO_2 and were detached with trypsin-EDTA solution.

2.4. Animal models

All animal experiments were conducted in compliance with the national legislation on laboratory animals' protection, and with the approval of the Ethics Committee for Animal Research (Lund University, Sweden). The experimental hosts were 6–8 week old male immunodeficient mice of BALB/c-nu and NMRI-nu strains, with the average weights of 25g and 30g, respectively. All mice were inoculated in the right flank by subcutaneous injection of $5–8\times10^6$ tumor cells in a 200μL cell suspension of 1:1 mixture of medium with Matrigel (BD Biosciences). We did not note any difference in levels of free, complexed and total PSA in these models (data not shown).

2.5. Bio-distribution studies

Bio-distribution studies were conducted to evaluate the uptake of ^{111}In-DTPA-5A10 in human prostate cancer xenograft models, as well as in non-tumor bearing mice. All mice received either 20μg or 50μg of ^{111}In-DTPA-5A10 [0.4–0.6 MBq (11–16 μCi)] in

approximately 100 μL PBS through tail-vein injection. The animals (n = 3–4 per group) were euthanized by intraperitoneal (i.p.) injection of Ketalar-Rompun solution (20 μL of solution per gram of body weight; Ketalar, 10 mg/ml; Rompun 1 mg/ml; from Pfizer and Bayer Animal Health, respectively) at 4, 24, 48, 72 and 168 hours post-injection. Blood was immediately harvested by cardiac puncture. Twelve tissue types (including tumor) were removed from each animal and placed in plastic 20 mL vials (Zinsser Analytic). After weighing, their ^{111}In radioactivity was assayed using a NaI(TI) well counter (1480 Wizard, Wallac). The mass of tracer injected into each animal was measured and used to determine the count rate by comparison with a standard syringe of ^{111}In-DTPA-5A10 with known activity and mass. Count data were corrected for background as well as physical decay. The tissue uptake was calculated as percentage injected activity per gram tissue (%IA/g) or as percentage injected activity (%IA).

2.6. Specificity of in vivo binding

Competitive inhibition (blocking) studies were performed *in vivo* to investigate the specificity of ^{111}In-DTPA-5A10 binding with PSA. A 40-fold excess (800μg) of unlabeled 5A10 was added to the ^{111}In-DTPA-5A10 (20μg) formulation to compete with its uptake in NMRI-nu mice with PSA-positive LNCaP tumors. In another experiment, ^{111}In-DTPA-5A10 was inoculated in PSA-negative xenografts (DU145 cells) and its uptake measured 72 hours post-injection to assess specificity of binding.

2.7. FcRn Blocking

To evaluate the effect of FcRn blockade on the bio-distribution of ^{111}In-DTPA-5A10, 1 mg/g body weight of human IgG1 non-specific for PSA was administered by intraperitoneal injection just before the radiotracer was injected (20μg per mouse, i.v.) to LNCaP-bearing NMRI-nu mice (n = 4). The mice were euthanized and tissues were collected 72 hours post injection. It should be noted that the dose of IgG1 was chosen to match that of IgG therapy for patients with humoral autoimmune disease [13].

2.8. Statistical analysis

Data was analyzed by using the unpaired, 2-tailed student t test (Excel, Microsoft). Differences at the 95% confidence level ($P < 0.05$) were considered to be statistically significant. Figures were produced with GraphPad Prism v.4 (GraphPad Software). All biodistribution data are shown as an average %IA/g of 3–4 animals ± standard errors of the mean [14] unless otherwise stated.

3. RESULTS

3.1. Radiolabeling and stability

We obtained a repeatable radiolabeling yield with ^{111}In-DTPA-5A10 of approximately 50% (n = 3). The radiochemical purity of the tracer after NAP-5 purification was greater than 99%, with a specific activity of 0.020–0.030 MBq/μg. There was no statistical difference in serum obtained from the NMRI-nu and BALB/c-nu mice after incubation of ^{111}In-DTPA-5A10 at 37°C (P = 0.83). The radiochemical purity of the conjugate decreased at 72 hours to 68 ± 12% and 71 ± 17% in NMRI-nu and BALB/c-nu serum, respectively.

3.2. Binding specificity

When the labeled conjugate was injected intravenously (i.v.) along with an excess of cold antibody in order to test antigen specificity, the tumor uptake decreased significantly. At 48 hours post-injection, tumor accumulation was 16 ± 4.3 %IA/g in mice which received a blocking dose of 5A10 along with ^{111}In-DTPA-5A10, compared to 37 ±16 %IA/g in mice who received only ^{111}In-DTPA-5A10 (Fig. 1A). As expected, tumor tissue from mice bearing PSA-negative DU145 xenografts that received 50 μg of ^{111}In-DTPA-5A10 showed little ($P < 0.05$) avidity for the tracer, 72 hours post-injection (Fig. 1B).

3.3. Bio-distribution in tumor models

Tissue bio-distribution of ^{111}In-DTPA-5A10 in LNCaP tumor–bearing NMRI-nu mice (intact B cells, increased NK cells and absent T cells) and BALB/c-nu mice (intact B and NK cells but with deficient T cells) models were performed to assess how the host immunodeficiency profile affected the uptake of this tracer. We also investigated if escalating the given dose of the tracer had a significant effect on bio-distribution.

The LNCaP-bearing NMRI-nu mice showed a 6-fold increase in tumor accumulation of the tracer from 24 h (8.8 ± 2.1 %IA/g) to its peak at 72 h (52 ± 10 %IA/g) (Fig. 2). The radioactivity measurements in the blood stayed constant over time, at approximately 13 ± 0.80 %IA/g and 14 ± 0.54 %IA/g at 24 h and 72 h, respectively. Thus the tumor-to-blood ratio increased from 0.68 at 24 h to 3.8 at 72 h.

The kinetics of tumor accumulation of the tracer in LNCaP-bearing BALB/c-nu mice were substantially different; tumor uptake of 19±13 %IA/g at 24 hours increased to only 24±11 %IA/g at 72 h. In addition, the radioactivity was continuously cleared from the blood circulation over time. The tumor-to-blood ratio was 0.62 at 24 h increasing to 2.1 at 72 h.

We also noted a significant difference ($P < 0.05$) in the liver accumulation of ^{111}In-DTPA-5A10 between the strains; hepatic uptake was 3.5 %IA/g in the NMRI-nu compared to 26 %IA/g at 72 h in the BALB/c-nu mice (Fig. 3A, B). The liver-to-blood ratio was considerably higher in the LNCaP-bearing BALB/c-nu compared to the NMRI-nu. However, the liver-to-blood ratio increased over the entire study duration (i.e. 168 h) in both strains (Table 1).

Overall, ^{111}In-DTPA-5A10 showed low accumulation in host tissues (GI tract, salivary glands, muscle, bone, brain and testes) though the activity was somewhat increased in highly vascularized organs (liver, heart, lung, spleen and kidneys). Except for tumor and liver tissue, tissue activity was lower than blood activity (Tables 1 and 2). Dose escalation (in tumor-bearing NMRI-nu) from 20 μg to 50 μg of ^{111}In-DTPA-5A10 had no significant ($P = 0.69$) effect on either tumor uptake or accumulation of the tracer in organs such as the liver (Fig. 1B).

3.4. Bio-distribution in naïve immunodeficient mice

In order to evaluate the effect of the presence of the tumor antigen on tissue kinetics, we looked at the tissue bio-distribution in naïve BALB/c-nu mice. This mouse strain had the

highest uptake of the radiolabeled antibody in normal organs. However, the accumulation of ^{111}In-DTPA-5A10 in naïve mice was lower in all organs measured, compared to LNCaP bearing BALB/c-nu mice. The blood and organ distribution kinetics of the tracer were also altered in tumor-bearing mice compared with the naïve mice (Fig. 4A). Remarkably, liver activity was 5-fold lower compared with tumor-bearing BALB/c-nu mice.

3.5. FcRn Blocking

FcRn saturation decrease the half-life of IgG by obstructing the receptor that protects IgG from rapid catabolism [15,16]. We used this strategy to determine the specific effect on the bio-distribution of ^{111}In-DTPA-5A10 in tumor-bearing model with the slowest catabolic rate; the NMRI-nu mice. There was no significant change in tumor accumulation ($P = 0.81$), but FcRn blocking significantly affected the residence time with reduced blood levels (6.2±1.9 %IA/g), at 72 hours, and increased spleen and salivary gland activity (Fig. 4B).

4. DISCUSSION

Cancer models using immunodeficient rodents are important tools for preclinical *in vivo* evaluation of molecular imaging probes. Small animals are convenient for laboratory investigation, and valuable models have been established that resemble human disease. Although the primary aim in testing a new probe in an animal model is to gain information on the specificity and extent of uptake at a disease site, the test may also elucidate additional factors that determine the overall utility of the tracer. This includes the percentage of the injected probe that aggregates non-specifically in healthy organs, and the rate and routes of clearance. Uptake in the liver and spleen has commonly been observed for radiolabeled antibodies. This is generally considered to be the result of the passive (i.e. mechanical) clearance of these radio-immunoconjugates. However, while investigating derived antibody conjugates in different disease models, we found that the presence and extent of immunodeficiency in the host strain critically affected the hepatic uptake of IgG1-based tracers. Although we found several reports on the clearance rate of different IgG subclasses and putative correlations to endogenous levels of antibodies in different rodents strains, we found little extant literature to elucidate the effect of the host's immunological profile on tracer bio-distribution and kinetics [2,3].

We have previously demonstrated that ^{89}Zr-DFO-5A10, an IgG1-based PET tracer, specifically localizes at prostate tumors [4]. However, ^{89}Zr-DFO-conjugated antibodies are naturally eliminated by the liver. Thus we initiated this study to evaluate a new construct, ^{111}In-DTPA-5A10. This tracer has clinical relevance as a SPECT agent and potential use as a targeted Auger electron therapy for metastatic prostate cancer. The fact that PSA is a protein exclusively expressed in human tissue pointed to fPSA-targeting as a model well suited to evaluate the effect of mouse models on tracer uptake. We thus chose ^{111}In-DTPA-5A10 to systematically investigate the distribution of a tracer in two murine systems with subtly different immunological profiles.

In vitro, ^{111}In-labeled antibody was moderately stable at 37 °C in both serum obtained from BALB/c-nu and NMRI-nu mice. This test was done to eliminate the possibility that any strain-specific serum proteins could cause the difference in bio-distribution noted between

the two strains. *In vivo*, using LNCaP xenografts, ^{111}In-DTPA-5A10 showed a robust, tumor-specific accumulation with low uptake in background organs compared to the blood activity in both strains. The presence of the antigen was required for high tumor uptake, as demonstrated in the lower accumulation in non-PSA-expressing DU145 tumors. However, the tumor uptake was markedly decreased in BALB/c-nu mice, in comparison to the NMRI-nu strain.

Although we are currently investigating this phenomenon, a putative explanation is that more tracer is trapped within the liver decreasing the amount of circulating antibodies for tumor targeting. We initially hypothesized that the lower blood volumes of the smaller BALB/c-nu mice could be a contributing factor. However, doubling the dose of antibody in the NMRI-nu strain did not cause a corresponding increase in hepatic accumulation. Instead, we correlated this observation to the clearance of high molecular weight complexes formed from 5A10, fPSA and antigen/antibody binders such as endogenous antibodies. This is a plausible theory supported by the finding that injection of ^{111}In-DTPA-5A10 into naïve BALB/c-nu mice (without PSA expression) resulted in altered blood clearance kinetics and a significantly lower uptake in several organs including the liver. We did not find any significant difference in the ratios of free and total PSA in blood between the models. Therefore, it is unlikely that the difference in liver uptake is due to an increased elimination of ^{111}In-DTPA-5A10 that has bound to inactive PSA (unbound to serine protease inhibitors) in the blood circulation.

Previous publications have suggested that CD64 (FcγRI) could potentially be a capacitating factor for elimination of IgG2a [3]. However, 5A10 is a mouse IgG1 antibody, a subclass that cannot bind FcγRI. We therefore reasoned that the difference between liver and tumor uptake in the two strains could therefore be due to FcRn activity which would be able to sequester administered tracer. It has been demonstrated that by inhibiting the FcRn it is possible to lower the contribution to background activity from FcRn binding. In our work, we did not observe a significant increase in the liver uptake or decrease in animal retention of activity following FcRn inhibition, as previously reported by Jaggi et al [16]. This effect of FcRn inhibition might be specific to both the target and the mouse model. Further, in our FcRn blocking experiments we used non-specific human IgG1, which unlike mouse IgG1 is functionally homologous to mouse IgG2a/b with ability to a bind FcγRI [17]. We are able to therefore rule out FcγRI as a factor that importantly affects elimination of 5A10.

To this end, we observed that the difference of antibody tracer distribution within murine systems is multifactorial: it can be attributed to the distribution of myeloid cells, efficiency of the reticulo-endothelial system and NK cells as well as the difference in the expression of receptors (i.e., FcRn), which can be unique to a particular mouse model. Nevertheless, efficient and robust pre-clinical screening of antibody-based imaging should be carried out in multiple mouse models.

5. CONCLUSIONS

The development of advanced imaging agents to detect and monitor disseminated prostate cancer is an area of considerable importance. The interpretation of data derived from the

preclinical evaluation of promising compounds often overlooks the immunological background and strain of the mouse model used when demonstrating or optimizing such tools. The present study has shown that the use of different mouse models, even with slight dissimilarity in immunological profile, is a capacitating factor that can potentially bias the verdict of a tracer. The host immune system has a substantial impact on both tumor uptake as well as elimination of the radiotracer. This work has implications for the further development of 5A10-based imaging as well as of other therapeutic compounds targeting fPSA, and offers some important considerations for preclinical evaluation of all targeted agents.

Acknowledgments

We wish to thank Anna Åkesson and Susanne Strömblad at the Department of Medical Radiation Physics for technical assistance. DLJT was supported by the Steven Wynn Young Investigator Award, and DU by the David H Koch Young Investigator Award, both of the Prostate Cancer Foundation. In addition, this study was performed with generous support from the Swedish Cancer Society (project no. 11-0624), the Swedish Science Council, Mrs. Berta Kamprad's Foundation, Gunnar Nilsson's Foundation, the ALF Foundation of the Medical Faculty of Lund University and Sidney Kimmel Center for Prostate and Urologic Cancers, David H. Koch through the Prostate Cancer Foundation, the National Institute for Health Research (NIHR) Oxford Biomedical Research Centre Program.

References

1. Pressman D. The development and use of radiolabeled antitumor antibodies. Cancer research. 1980; 40:2960–4. [PubMed: 6994879]
2. Waldman TA, Strober W. Metabolism of immunoglobulins. Progress in Allergy. 1969; 13:1–110. [PubMed: 4186070]
3. Reddy N, Ong GL, Behr TM, Sharkey RM, Goldenberg DM, Mattes MJ. Rapid blood clearance of mouse IgG2a and human IgG1 in many nude and nu/+ mouse strains is due to low IgG2a serum concentrations. Cancer immunology, immunotherapy. 1998; 46:25–33. [PubMed: 9520289]
4. Ulmert D, Evans MJ, Holland JP, Rice SL, Wongvipat J, Pettersson K, et al. Imaging androgen receptor signaling with a radiotracer targeting free prostate-specific antigen. Cancer discovery. 2012; 2:320–7. [PubMed: 22576209]
5. Thorek DL, Evans MJ, Carlsson SV, Ulmert D, Lilja H. Prostate-specific kallikreinrelated peptidases and their relation to prostate cancer biology and detection. Established relevance and emerging roles. Thrombosis and haemostasis. 2013; 110:484–92. [PubMed: 23903407]
6. Lilja H, Ulmert D, Vickers AJ. Prostate-specific antigen and prostate cancer: prediction, detection and monitoring. Nature reviews Cancer. 2008; 8:268–78.
7. Lawrence MG, Lai J, Clements JA. Kallikreins on steroids: structure, function, and hormonal regulation of prostate-specific antigen and the extended kallikrein locus. Endocrine reviews. 2010; 31:407–46. [PubMed: 20103546]
8. Stege RH, Tribukait B, Carlstrom KA, Grande M, Pousette AH. Tissue PSA from fine-needle biopsies of prostatic carcinoma as related to serum PSA, clinical stage, cytological grade, and DNA ploidy. The Prostate. 1999; 38:183–8. [PubMed: 10068342]
9. Savblom C, Malm J, Giwercman A, Nilsson J-A, Berglund G, Lilja H. Blood levels of free-PSA but not complex-PSA correlates to prostate releases of PSA in semen in young men, while blood levels of complex, but not free-PSA increase with age. The Prostate. 2005; 65:66–72. [PubMed: 15880475]
10. Christensson A, Laurell CB, Lilja H. Enzymatic activity of prostate-specific antigen and its reactions with extracellular serine proteinase inhibitors. European journal of biochemistry / FEBS. 1990; 194:755–63. [PubMed: 1702714]

11. Lilja H, Christensson A, Dahlén U, Matikainen MT, Nilsson O, Pettersson K, Lövgren T. Prostate-specific antigen in serum occurs predominantly in complex with alpha 1-antichymotrypsin. Clin Chem. 1991 Sep; 37(9):1618–25. [PubMed: 1716536]
12. Pettersson K, Piironen T, Seppala M, Liukkonen L, Christensson A, Matikainen MT, et al. Free and complexed prostate-specific antigen (PSA): in vitro stability, epitope map, and development of immunofluorometric assays for specific and sensitive detection of free PSA and PSA-alpha 1-antichymotrypsin complex. Clinical chemistry. 1995; 41:1480–8. [PubMed: 7586521]
13. Hansen RJ, Balthasar JP. Mechanisms of IVIG action in immune thrombocytopenic purpura. Clinical laboratory. 2004; 50:133–40. [PubMed: 15074465]
14. Haseman MK, Rosenthal SA, Polascik TJ. Capromab Pendetide imaging of prostate cancer. Cancer biotherapy & radiopharmaceuticals. 2000; 15:131–40. [PubMed: 10803318]
15. Hansen RJ, Balthasar JP. Intravenous immunoglobulin mediates an increase in antiplatelet antibody clearance via the FcRn receptor. Thrombosis and haemostasis. 2002; 88:898–9. [PubMed: 12529736]
16. Jaggi JS, Carrasquillo JA, Seshan SV, Zanzonico P, Henke E, Nagel A, et al. Improved tumor imaging and therapy via i.v. IgG-mediated time-sequential modulation of neonatal Fc receptor. The Journal of clinical investigation. 2007; 117:2422–30. [PubMed: 17717602]
17. Unkeless JC, Eisen HN. Binding of monomeric immunoglobulins to Fc receptors of mouse macrophages. The journal of experimental medicine. 1975; 142:1520–33. [PubMed: 1194857]

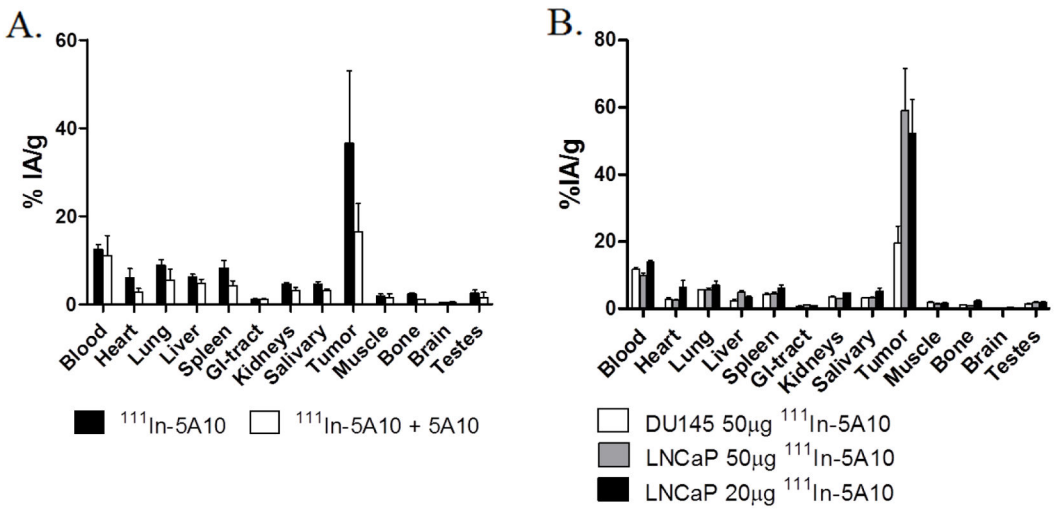

Figure 1. Specificity of ^{111}In-DTPA-5A10 uptake and dose escalation in NMRI-nu mice

A. A significant decrease in the tumor-bound activity was seen when co-administered 800 µg non-labeled antibody with ^{111}In-DTPA-5A10. The tumor-bound activity was 36.6 ± 16.4 %IA/g for administration of ^{111}In-DTPA-5A10 alone and 16.4 ± 6.4 %IA/g for co-administration. Tissues were harvested at 48 h post-injection. **B.** A significantly lower uptake ($P < 0.05$) is shown in non-PSA-expressing DU145 xenografts, compared to LNCaP xenografts. Increased antibody mass from 20 µg to 50 µg did not significantly alter tissue bio-distribution in LNCaP xenografts. Tissues were harvested at 72 h post-injection.

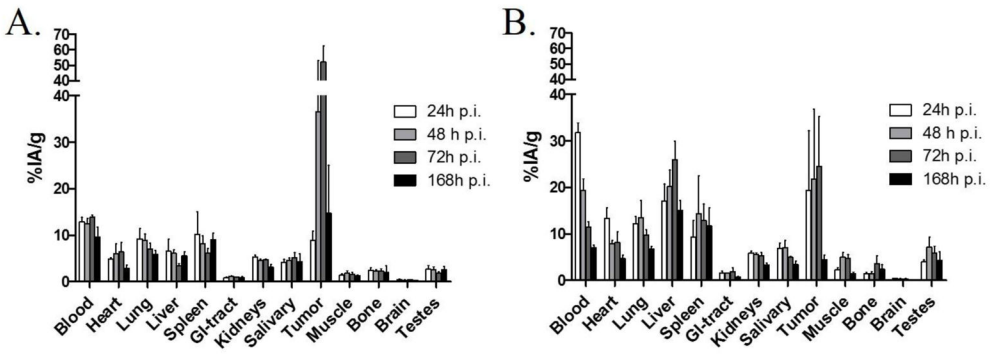

Figure 2. Bio-distribution of ^{111}In-DTPA-5A10 in two different mouse strains with different host immunodeficiency profiles bearing LNCaP xenografts

A. LNCaP tumor–bearing NMRI-nu (with intact B cells, increased NK cells and absent T cells). **B.** LNCaP tumor–bearing BALB/cnu (with intact B and NK cells but with deficient T cells) mice.

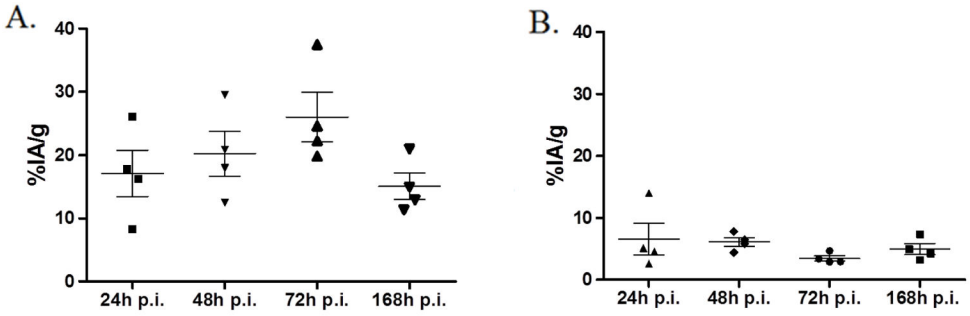

Figure 3. Liver uptake over time in NMRI-nu with s.c. LNCaP xenografts in comparison to BALB/c-nu mice with s.c. LNCaP xenografts

A. BALB/c-nu mice **B.** NMRI-nu mice

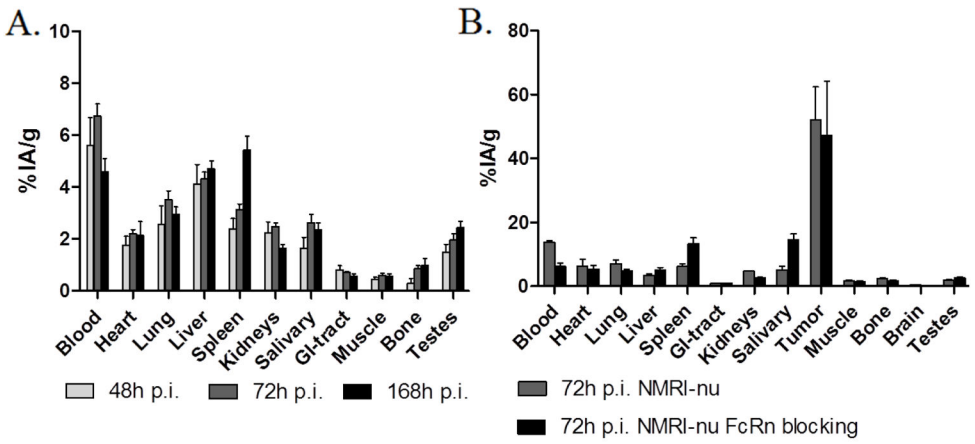

Figure 4. Role of tumor antigen presence on radio-immunoconjugate distribution; and FcRn blocking

A. Bio-distribution of ^{111}In-DTPA-5A10 in tumor naïve BALB/c-nu mice showing a significantly lower accumulation in all organs compared to tumor bearing BALB/c-nu mice (Fig. 2B). **B.** The effect of nonspecific IgG1 mediated FcRn blocking on biodistribution of ^{111}In-DTPA-5A10 in LNCaP xenografted NMRI-nu mice. Tumor uptake was not affected, but accelerated blood clearance and an increased accumulation in the spleen and salivary glands were observed. Tissues were harvested at 72 h post tracer injection.

Table 1

Organ-to-Blood Ratios

Tissue	Organ/Blood ±SEM			
	24h (*n* = *3*)	48h (*n* = *4*)	72h (*n* = *4*)	168h (*n* = *3*)
NMRI-nu				
Tumor	0.85±0.14	2.73±0.99	3.73±0.69	1.26±0.65
Heart	0.37±0.04	0.46±0.11	0.45±0.12	0.30±0.01
Lung	0.75±0.21	0.71±0.08	0.50±0.08	0.64±0.07
Liver	0.55±0.27	0.51±0.09	0.25±0.03	0.67±0.24
Spleen	0.86±0.52	0.64±0.08	0.44±0.05	1.02±0.26
GI Tract	0.07±0.02	0.10±0.02	0.07±0.00	0.09±0.00
Kidneys	0.39±0.03	0.38±0.02	0.35±0.01	0.34±0.02
Salivary glands	0.30±0.06	0.37±0.03	0.37±0.06	0.48±0.21
Muscle	0.12±0.03	0.14±0.03	0.11±0.03	0.16±0.04
Bone	0.13±0.06	0.19±0.04	0.17±0.03	0.33±0.03
Brain	0.04±0.00	0.03±0.00	0.03±0.00	0.03±0.01
Testes	0.23±0.08	0.20±0.04	0.14±0.03	0.28±0.08
BALB/c-nu				
Tumor	0.82±0.54	1.51±1.18	1.46±0.59	0.63±0.12
Heart	0.53±0.15	0.44±0.08	0.69±0.28	0.74±0.21
Lung	0.55±0.17	0.69±0.14	1.01±0.41	1.01±0.14
Liver	0.80±0.32	1.03±0.07	1.93±0.56	2.20±0.28
Spleen	0.46±0.17	0.95±0.66	0.92±0.37	1.60±0.54
GI Tract	0.07±0.03	0.09±0.01	0.16±0.10	0.11±0.01
Kidneys	0.26±0.07	0.30±0.05	0.37±0.08	0.46±0.03
Salivary gland	0.28±0.06	0.37±0.09	1.45±1.14	0.48±0.06
Muscle	0.11±0.03	0.27±0.07	0.34±0.09	0.21±0.05
Bone	0.07±0.03	0.08±0.04	0.28±0.17	0.35±0.14
Brain	0.02±0.01	0.02±0.01	0.03±0.01	0.02±0.01
Testes	0.18±0.04	0.36±0.08	0.36±0.03	0.60±0.24

Table 2

Tumor-to-Organ Ratios

Tissue	Tumor/Organ ±SEM			
	24h (*n* = *3*)	48h (*n* = *4*)	72h (*n* = *4*)	168h (*n* = *3*)
NMRI-nu				
Blood	0.85±0.14	2.73±0.99	3.73±0.69	1.26±0.65
Heart	2.35±0.45	5.68±1.24	9.69±2.86	4.21±2.19
Lung	1.58±0.83	4.03±1.31	7.43±0.74	2.16±1.25
Liver	2.56±1.28	6.46±2.85	15.4±3.32	2.97±2.09
Spleen	2.33±1.41	4.24±1.23	8.72±2.15	1.48±0.87
GI Tract	16.1±7.09	32.1±14.4	55.9±12.1	13.2±6.51
Kidneys	2.24±0.57	7.57±2.96	11.0±2.19	3.95±2.21
Salivary glands	3.26±1.18	7.51±2.54	10.9±2.92	4.06±2.63
Muscle	8.28±2.31	19.3±5.08	41.2±13.1	12.1±8.92
Bone	4.79±3.18	17.7±9.76	23.3±4.22	13.0±8.21
Brain	22.8±4.60	94.6±30.6	136±33.9	46.9±30.60
Testes	4.89±1.90	13.0±3.31	35.1±13.3	6.07±4.09
BALB/c-nu				
Blood	0.82±0.54	1.51±1.18	1.46±0.59	0.63±0.12
Heart	2.49±2.04	2.62±1.69	4.05±2.40	1.11±0.41
Lung	1.57±1.04	1.98±1.33	2.41±1.12	0.65±0.13
Liver	1.99±1.67	1.58±1.26	1.04±0.47	0.29±0.04
Spleen	2.91±1.41	1.29±0.24	2.29±0.98	0.65±0.28
GI Tract	11.4±6.39	14.2±9.96	17.6±9.20	5.69±1.11
Kidneys	2.99±1.86	3.86±2.59	4.09±1.39	1.35±0.23
Salivary gland	2.61±1.60	4.05±2.99	3.64±2.38	1.34±0.22
Muscle	8.03±4.71	4.30±2.48	6.29±2.88	3.47±0.92
Bone	16.3±11.8	13.3±4.53	12.4±6.11	2.54±0.87
Brain	47.5±30.7	49.9±26.9	86.5±39.9	20.8±2.58
Testes	4.99±3.32	4.17±2.77	4.06±1.45	1.28±0.22